Physica B 174 (1991) 396–402
North-Holland

Fundamental and applied neutron interferometry

J. Summhammer and A. Zeilinger
Atominstitut der Österreichischen Universitäten Schüttelstraße 115, A-1020 Vienna, Austria

We present three neutron interferometry experiments on fundamental questions and one new application made possible with the grating interferometer for very cold neutrons. The fundamental experiments are: recent results with very strong attenuation in one beam in the interferometer; an experiment which is just being started to observe multi-photon exchange between neutron and an oscillating magnetic field; and a proposal for the measurement of the scalar Aharanov–Bohm effect. With applications, the very cold neutron interferometer opens the possibility to observe the local field correction to the neutron refractive index in media, which should become observable as a Fizeau phase shift.

1. Introduction

Today, there are three typical kinds of neutron interferometers in operation: an interferometer based on a combination of mirrors and diffraction gratings for neutrons of wavelength $\lambda = 3.15$ Å [1], a grating interferometer for very cold neutrons with $\lambda = 100$ Å [2], and crystal interferometers of various designs using thermal neutrons [3]. In this paper we will present four selected experiments, results as well as proposals, employing a crystal interferometer and the grating interferometer of ref. [2].

Crystal interferometers are cut from a monolithic block of single crystal silicon with several slabs jutting up from a common base. These slabs are used for beam splitting and recombination by means of Bragg and/or Laue reflection from a suitable lattice plane (here, the 220-plane exclusively). Incident neutron energies are in the thermal spectrum to give Bragg angles around 30° and hence beam separations of several centimeters.

2. Fundamental experiments

In these experiments the interferometer is used to investigate properties of the neutron as a quantum mechanical particle. There have been a series of experiments on the influence of the earth's gravity and rotation [4] on the phase of the neutron's wave function, on interference in non-inertial reference frames [5], on the phase transformation under rotation of the neutron's spin [6–8], on the superposition of different energy states of the neutron [9] and on the decrease of interference with increasing absorption in one path of the interferometer [10, 11].

2.1. Strong absorption in one beam path

The absorption experiments have recently been refined to incorporate a very high attenuation in one beam path [12]. A sketch of the generic situations is shown in fig. 1. In the case of stochastic absorption (cf. fig. 1(a)), as in a homogeneous partial absorber (here a solid slab or a liquid solution), the wave function of the neutron in that path is reduced by an overall factor $\sqrt{\alpha}$, where α is the transmission probability through the absorber. Hence the intensity at detector O (that at detector H is analogous) turns out to be:

$$I_O(\alpha, \chi) = |\psi_R + \sqrt{\alpha}\psi_L e^{i\chi}|^2 = |\psi_R|^2[1 + \alpha + 2\sqrt{\alpha}\cos(\chi)]. \quad (1)$$

Here, ψ_R and ψ_L denote the wavefunction at

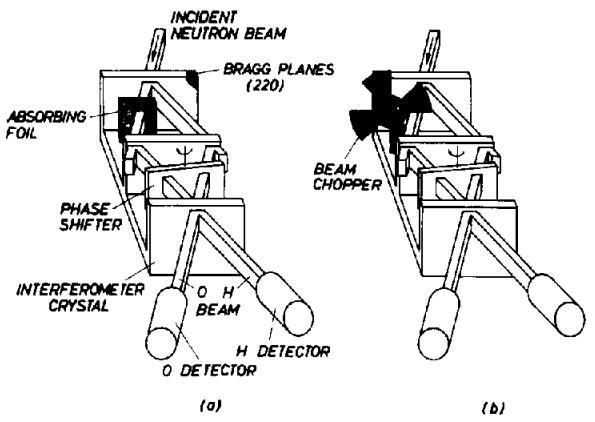

Fig. 1 (a) Attenuation of the left beam by absorbing gold or indium foils, by a Gd-solution, or by a Si single crystal in almost Bragg condition. Wavelength $\lambda = 1.97$ Å, $\Delta\lambda/\lambda = 1\%$. (b) Attenuation of the left beam by a chopper. Rotation frequency: 4 Hz. In the experiment three different chopper disks were used with effective transmissions of around 25%, 50% and 75%, respectively (see fig. 2).

detector O due to the left and right path, respectively, and χ represents the variable phase shift of the left path relative to the right one due to the phase plate plus a possible constant phase induced by the absorber. In the calculation we made use of the identity $\psi_L = \psi_R$ which is true for an ideal crystal interferometer of the type shown in fig. 1. Note that the reduction of the interference term goes as the square root of the transmission probability through the absorber. This yields a relatively strong interference even when the left path is almost fully blocked. In recent experiments the factor α was made as small as 0.00032(18) by means of a Si crystal (instead of an absorber) which reflected most of the beam in another direction where it was absorbed [12]. The observed amplitude of interference was 0.0127(30) relative to that of the interferometer without any absorber (fig. 2). There have been a number of theoretical papers dealing with the complementarity of partial path information and interference amplitude with respect to this experiment [13–17], or similar optical ones [18].

Another way of attenuating a neutron beam is by chopping it (see fig. 1(b)) or reducing its cross section in some manner. We define this as deterministic attenuation since the absorbing sections are assumed completely black [10]. As an example think of a shutter which blocks the left path periodically for a fraction $1 - \alpha$ of the total measuring time, and opens the path for a fraction α. The intensity at detector O is then:

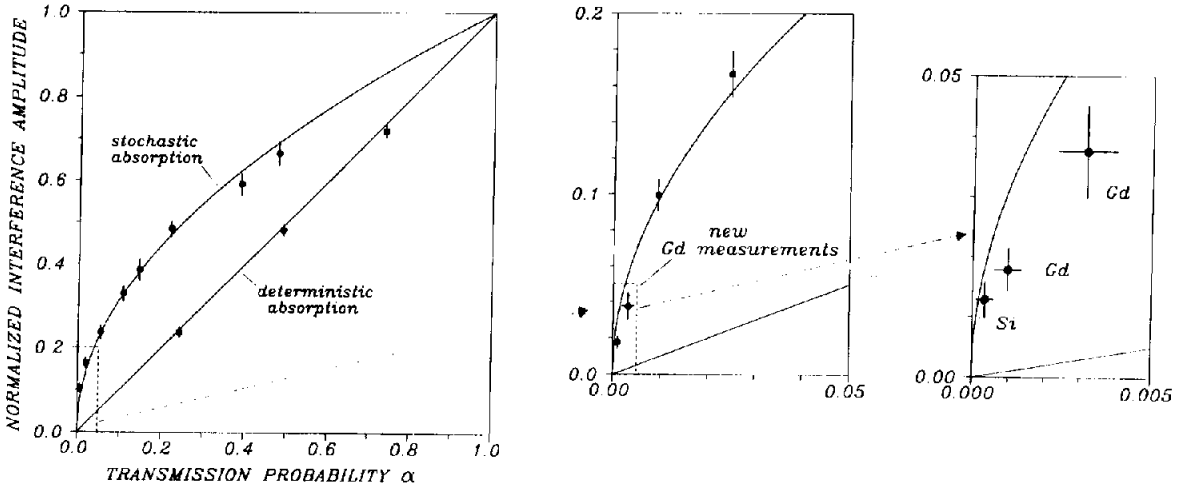

Fig. 2. Normalized interference amplitude as a function of transmission through the absorber region. Left: results with gold or indium foils (stochastic) and with a chopper (deterministic). The curves are not fits, but theoretical predictions. Center: results with highly absorbing aqueous solutions of a Gd-salt. Right: same as center, but also with results of Si-crystal in almost Bragg condition which reflected most of the beam into a beam stop and thus had very little transmission.

$$I_O(\alpha, \chi) = \alpha|\psi_R + \psi_L e^{i\chi}|^2 + (1-\alpha)|\psi_R|^2$$
$$= |\psi_R|^2[1 + \alpha + 2\alpha\cos(\chi)]. \quad (2)$$

The reduction of the interference pattern now is directly proportional to the average transmission probability through the left path (fig. 2). This in spite of the fact that the mean number of neutrons that are taken out of the left beam can be made the same in the stochastic and the deterministic experiments. It should be mentioned that the summing of the intensities of the situations 'left path open' and 'left path closed' in eq. (2) is intuitively clear with a slow chopper. A more correct analysis would describe the left beam behind the chopper as a series of wave-packets [10, 19], while before the chopper a plane wave can be assumed just as in the right path. Then these wave packets are composed of the superposition of many plane waves of different energies, the difference being in multiples of the frequency of opening and closing of the beam. When measuring the time averaged interference pattern only those energy components contribute, which are the same in the left and the right paths. This explains why in this case the interference pattern is smaller than in the stochastic case.

2.2. *Multi-photon exchange between neutron and electromagnetic field*

In interferometry with polarized neutrons the Rabi spin flip device has so far been used to invert the neutron spin in one [8] or in both paths [9]. There, the exchange of one photon between neutron and electromagnetic field was exploited to invert the spin state and simultaneously change the energy of the neutron by just the energy of a photon (usually in the 50 to 100 kHz range). However in the general case a neutron traversing a region with a time dependent electromagnetic field can exchange (emit or absorb) any number of photons with a corresponding change of its energy. This need not necessarily be accompanied by a spin flip [20, 21]. In the usual spin flip setup, the static magnetic guide field B_0 and oscillating field B_{rf} are orthogonal to each other. The neutrons traverse a region of space with a magnetic field

$$\boldsymbol{B}(t) = [B_{rf}\cos(\omega_{rf}t), 0, B_0]. \quad (3)$$

Absorption or emission of an odd number of photons leads to a spin flip, whereas an exchange of an even number of photons preserves the spin state. In general a transition from an initial neutron state ψ_i to the final state ψ_f in a field region containing a time dependent component periodic with ω_{rf} can be written as

$$\psi_i = \begin{pmatrix} \exp(i\boldsymbol{k}\boldsymbol{r} - iEt/\hbar) \\ 0 \end{pmatrix} \rightarrow$$
$$\psi_f = \begin{pmatrix} \sum_n c_n \exp(i\boldsymbol{k}_n\boldsymbol{r} - i(E + n\hbar\omega_{rf})t/\hbar) \\ \sum_n d_n \exp(i\boldsymbol{k}_n\boldsymbol{r} - i(E - n\hbar\omega_{rf})t/\hbar) \end{pmatrix}. \quad (4)$$

Here, the initial state ψ_i was assumed as a plane wave with spin state $+z$. The amplitudes c_n represent the transition probabilities to an energy state where n photons were absorbed or emitted (depending on the sign of n) but the spin state remained unchanged. The d_n's represent the amplitudes for absorption or emission of n photons and simultaneous transition to the $-z$ spin state. The index n goes from a negative minimum value given by the original energy E of the neutron to plus infinity. The transition amplitudes reach a maximum at n_{max} which is given approximately by the maximum difference in Zeeman energy between the neutron's entrance and exit from the field region, divided by the photon energy.

If such a general transition is induced in one path of the interferometer it is possible to measure the c_n and d_n in magnitude and phase by superposition with the beam in the other path which remains in the initial state. The necessary setup is sketched in fig. 3. With the devices F_1 and F_2 switched off one measures a superposition of the $+z$ components of the left and the right path, whereas when they are switched on the original state in the left path experiences a static spin turn and hence superposition of the $-z$

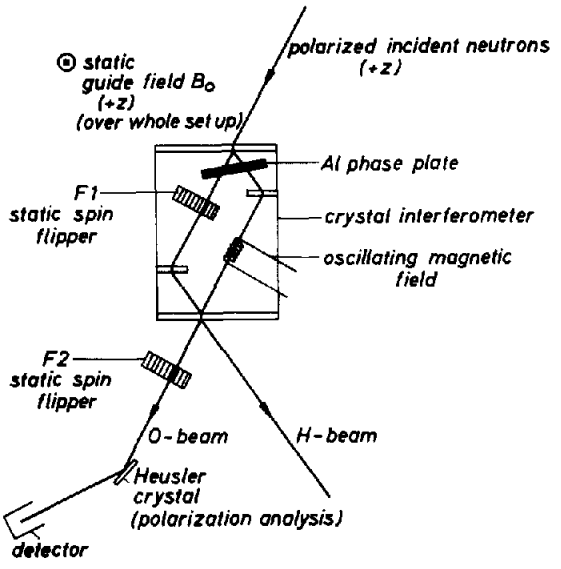

Fig. 3. Setup for experiment on the multi-photon exchange between neutron and the electromagnetic field to be performed at the ILL. For reasons of space a skew symmetric crystal interferometer will be used (see, e.g., ref. [9]). The frequencies of the oscillating magnetic field will be below 100 kHz, as exchange of several photons changes the neutron's momentum which in turn influences the reflectivity at subsequent crystal slabs due to Pendellösung-effects (see, e.g., refs. [7, 32]).

components is reached. Intensity is recorded as a function of time. Fourier analysis of the intensity yields the amplitudes c_n and d_n.

It is worthwhile to draw attention to conservation of angular momentum. When the neutron absorbs or emits one photon its spin is flipped conserving total angular momentum of photon plus neutron. When more photons are absorbed or emitted the process can be thought of as successive emissions/absorptions, each conserving the total angular momentum.

The situation is different when the oscillating field is parallel to the guide field, just weakly modulating it periodically in a region of space,

$$\boldsymbol{B}(t) = [0, 0, B_0 + B_{\mathrm{rf}} \cos(\omega_{\mathrm{rf}} t)] . \qquad (5)$$

A neutron with spin in an eigenstate of the guide field will not experience a spin flip when traversing this region. But it will in general exchange several photons with the field thus changing its energy by a discrete amount. Calculations show that the neutron can absorb or emit any number of photons [21]. Therefore the total angular momentum of neutron plus photon is not conserved, suggesting that the oscillating field as a whole, which is a coherent state of the electromagnetic field, has to be taken into consideration. In the present experiment such an arrangement will also be tested to determine the different transition amplitudes c_n, especially those with odd n, which should all vanish from the (wrong) point of view of conservation of angular momentum of just photon plus neutron.

An interesting side aspect of the proposed experiment is the change in reflectivity from one crystal plate to the next, when the neutron's kinetic energy has changed in between. This effect is due to the Pendellösung structure of reflection and transmission near the Bragg condition in a single crystal. With the absorption of two photons of 50 kHz and no spin flip the relative change in the neutron's wavelength is only $\Delta\lambda/\lambda \approx 10^{-8}$ for $\lambda = 1.9$ Å. Nevertheless this will lead to a change of reflectivity in the percent range, the change being approximately quadratic in $\Delta\lambda/\lambda$ [32]. In the arrangement of fig. 3 some intensity will be shifted from beam O to beam H or vice versa. For the proposed experiment this means that the amplitudes c_n and d_n as well as their relative phases as obtained from the Fourier analysis of the data will have to be corrected for this effect. In earlier experiments such a correction showed good agreement between experimental data and theoretical description [7, 32].

2.3. *Scalar Aharanov–Bohm effect*

This experiment will be performed with the grating interferometer for cold neutrons installed at the Institut Laue–Langevin [22]. It uses neutrons with a wavelength around 100 Å, corresponding to a velocity around 40 m/s and a kinetic energy around 8 μeV. Beam splitting and recombination is achieved by one-dimensional phase gratings etched into quartz glass with a periodicity of 2 μm. The depth of the etched

lines is such that for neutrons with $\lambda = 100$ Å the phase difference between paths through etched and non-etched lines, is $\pi/2$ for the first and third gratings and π for the second grating. The first-order diffraction at these gratings results in a beam geometry as shown in fig. 4. The length of the interferometer is currently 50 cm with a planned extension to 4 m. The beam separation at the second grating is currently around 1 mm. The interference pattern is obtained by scanning the third grating.

The magnetic Aharanov–Bohm effect is well demonstrated in electron interferometry [23, 24], while the electric one still awaits experimental verification. The latter demonstrates the role of the scalar potential. The experimental difficulty consists in the need to switch a voltage applied to a Faraday cage on and off while the electron is inside, a nontrivial problem due to the high velocities of electrons. Another obstacle is the beam separation of the order of only 100 μm in present electron interferometers [25]. The concept of the scalar Aharanov–Bohm effect can readily be extended to neutrons. The neutron must pass through a region in which a homogeneous magnetic field is switched on after the neutron has entered and is switched off before it exits. Hence the wave function is changed by an additional phase [26],

$$\Delta\varphi = \frac{\pm \int \mu \boldsymbol{B}(t)\, \mathrm{d}t}{\hbar}, \qquad (6)$$

the signs applying to the two different spin eigenstates in the field. This phase can only be detected by interference with an unperturbed beam, as no accelerating or decelerating forces act on the neutron during the process. This is in contrast to a static magnetic field, where the neutron is subject to such forces upon entrance to and exit from the region, permitting a measurement of the effect in a time of flight arrangement. In the proposed experiment the magnetic field will be generated by a current sheet between the two beams, the current being orthogonal to the interferometric plane. Therefore the two paths will be in opposite magnetic fields, which doubles the phase due to the scalar Aharanov–Bohm effect. The low neutron velocity affords switching on and off of the current with only a few kilohertz. Another advantage of performing the test with this interferometer is the large wavelength distribution of $\Delta\lambda/\lambda = 22\%$. The scalar Aharanov–Bohm effect is nondispersive. On the other hand, the phase shift accumulated in a static magnetic field is dispersive. An unambiguous demonstration of the effect can therefore be achieved by showing that the interference pattern for a certain field strength is still fully present when switching on after the neutron has entered and switching off before it leaves the field region, whereas interference vanishes when the field is kept static. For other fundamental tests which for the first time can be done with a very cold neutron interferometer of the envisioned final size of 4 m we refer to ref. [22].

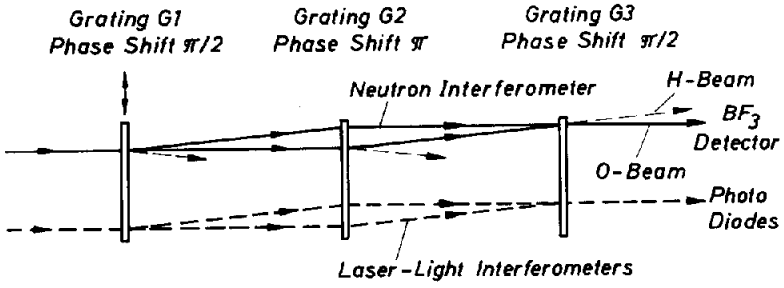

Fig. 4. Top view of very cold neutron interferometer. Beam splitting, refocusing and recombination at gratings G1, G2 and G3, respectively. Three laser interferometers at different heights for fine tuning utilize separate gratings etched on the same substrate as gratings for neutrons.

3. An applied experiment – local-field correction to the neutron optical potential

The neutron optical potential of a medium for thermal neutrons is to a very good approximation given by [27]

$$V = \frac{2\pi\hbar^2}{m} Nb\,, \tag{7}$$

where m is the neutron mass, N is the density of atoms in the medium and b is the average coherent scattering length per nucleus. This expression shows no dependence on energy. Therefore, there should be no neutron optical analog of the Fizeau effect, that is, there should be no phase shift when a neutron passes through a plane slab of a medium which itself moves parallel to its surface. This has been tested in a crystal interferometer with neutrons of $\lambda = 1.268$ Å [28]. There is, however, a correction to the neutron optical potential, which essentially consists in taking into account that the local field at an atomic site is comprised of the incident neutron wave plus the waves scattered from all the other atoms [29]. Then eq. (7) has to be rewritten as [27]:

$$V = \frac{2\pi\hbar^2}{m} Nb(1 - J)\,, \tag{8}$$

with

$$J = \frac{2\pi Nb}{k} \int_0^\infty [1 - g(r)] \sin(2kr)\, \mathrm{d}r\,.$$

Here, k is the incident neutron wave vector and $g(r)$ is the pair correlation function of the atoms in the medium. One notes that the optical potential is now a function of k and thus of the energy of the incident neutrons. Since the Fizeau phase shift depends on $\mathrm{d}V/\mathrm{d}E$ it should become manifest when this derivative reaches experimentally accessible values. This is the case with the grating interferometer of reference [2]. In the experiment with a crystal interferometer [28] one expected $|\mathrm{d}V/\mathrm{d}E| \approx 3 \times 10^{-12}$, while the experimental upper bound was 2.1×10^{-8}. In contrast, with neutrons of $\lambda = 100$ Å of the grating interferometer one expects [27] $\mathrm{d}V/\mathrm{d}E \approx -1.2 \times 10^{-8}$.

The proposed test will be performed in the following way: a phase plate of a suitable material (e.g., fused quartz as in ref. [28]) formed as a disk is inserted in one path of the interferometer and rotated around an axis parallel to the neutron beam. In this way the medium moves relative to the beam, but the surface of the disk does not. To compensate for the large phase shift already present when the disk is not rotated at all, an equivalent static phase plate is put into the other path. In this manner one avoids destruction of interference, which at high phase shifts occurs in this interferometer due to the dispersivity of the phase shift in combination with the relatively large wavelength spread of the incident beam. For lack of sufficient beam separation a nondispersive arrangement as sometimes used with crystal interferometers [30] cannot be applied here. The Fizeau phase shift will then be recorded as a function of the speed of the disk. This should give important information on the correction to the scattering length produced by local field effects [31].

An estimate of the achievable lower limit for $|\mathrm{d}V/\mathrm{d}E|$ is obtained as follows: Let the optical potential for the disk at rest be V. Then the phase shift through the material, relative to vacuum, is $\varphi = kDV/2E$, k being the vacuum wave number, E the neutron energy and D the path length through the disk. With the rotating disk, let k_r be the vacuum wave number as "seen" from a reference frame of atoms in the disk. Correspondingly, $E_r = \hbar^2 k_r^2/2m$. Hence the additional phase shift $\delta\varphi$ is given by $\delta\varphi/\varphi = [(E_r - E)/V\ (\Delta V/\Delta E)$. Now, $V \approx 10^{-7}$ eV and for a velocity of the disk of around 69 m/s, $E_r - E \approx 3E \approx 24\ \mu$eV. Assume now, conservatively, an accuracy of the phase shift measurements of $\Delta\varphi < 2\pi \times 10^{-2}$, a thickness of the disk of 1.7 cm (giving a phase shift of $2\pi \times 10^4$ in SiO_2). Then one should be able to set a lower limit, $|\Delta V/\Delta E| > 4 \times 10^{-9}$.

Acknowledgements

One of us (J.S.) would like to thank Professor H. Rauch for lending him material on the most recent results of absorption experiments in the interferometer. All experiments reported here are financially supported by the Austrian Fonds zur Förderung der wissenschaftlichen Forschung, project number S4201.

References

[1] A.I. Ioffe, V.S. Zabiyakin and G.M. Drabkin, Phys. Lett. A 111 (1985) 373.
[2] M. Gruber, K. Eder, A. Zeilinger, R. Gähler and W. Mampe, Phys. Lett. A 140 (1989) 363.
[3] G. Badurek, H. Rauch and A. Zeilinger, eds., Proc. Int. Workshop on Matter Wave Interferometry, Vienna 1987, Physica B 151 (1988).
[4] S.A. Werner, H. Kaiser, M. Arif and R. Clothier, Physica B 151 (1988) 22.
[5] U. Bonse and T. Wroblewski, Phys. Rev. Lett. 51 (1983) 1401.
[6] H. Rauch, A. Wilfing, W. Bauspiess and U. Bonse, Z. Phys. B 29 (1978) 281.
[7] J. Summhammer, G. Badurek, H. Rauch, U. Kischko and A. Zeilinger, Phys. Rev. A 27 (1983) 2523.
[8] G. Badurek, H. Rauch and J. Summhammer, Phys. Rev. Lett. 51 (1983) 1015.
[9] G. Badurek, H. Rauch and D. Tuppinger, Phys. Rev. A 34 (1986) 2600.
[10] J. Summhammer, H. Rauch and D. Tuppinger, Phys. Rev. A 36 (1987) 4447.
[11] H. Rauch and J. Summhammer, Phys. Lett. A 104 (1984) 44.
[12] H. Rauch, J. Summhammer, M. Zawisky and E. Jericha, Phys. Rev. A 42 (1990) 3726.
[13] W.M. de Muynck and H. Martens, Phys. Rev. A 42 (1990) 5079.
[14] D.M. Greenberger, Rev. Mod. Phys. 55 (1983) 875.
[15] A. Zeilinger, Physica B 137 (1986) 235.
[16] D.M. Greenberger and A. Yasin, Phys. Lett. A 128 (1988) 391.
[17] P. Mittelstaedt, A. Prieur and R. Schieder, Found. Phys. 17 (1987) 891.
[18] W.K. Wootters and W.H. Zurek, Phys. Rev. D 19 (1979) 473.
[19] J. Felber, R. Gähler and R. Golub, Physica B 151 (1988) 135.
[20] E. Muskat, D. Dubbers and O. Schärpf, Phys. Rev. Lett. 58 (1987) 2047.
[21] D.L. Haavig, R. Reifenberger, Phys. Rev. B 26 (1982) 6408.
[22] K. Eder, M. Gruber, A. Zeilinger, R. Gähler, W. Mampe and W. Drexel, Nucl. Instr. Meth. A 284 (1989) 171.
[23] Y. Aharanov and D. Bohm, Phys. Rev. 115 (1959) 485.
[24] A. Tonomura, Rev. Mod. Phys. 59 (1987) 639.
[25] F. Hasselbach, Z. Phys. B 71 (1988) 443.
[26] A. Zeilinger, J. Phys. (Paris) 45, Suppl. (1984) C3–213.
[27] V.F. Sears, Phys. Rev. A 32 (1985) 2524.
[28] M. Arif, H. Kaiser, S.A. Werner, A. Cimmino, W.A. Hamilton, A.G. Klein and G.I. Opat, Phys. Rev. A 31 (1985) 1203.
[29] V.F. Sears, Phys. Rep. 82 (1982) 1.
[30] H. Rauch, E. Seidl, D. Tuppinger, D. Petrascheck and R. Scherm, Z. Phys. B 69 (1987) 313.
[31] V.F. Sears, Z. Phys. A 321 (1985) 443.
[32] J. Summhammer, Doctoral Thesis (Technical University of Vienna, 1983, unpublished).